01 Jan 1991

Effects Of Sample Orientation On The Corrosion Of Zinc In Ammonium Sulfate And Sodium Hydroxide Solutions

D. Abayarathna

Edward Boyd Hale
Missouri University of Science and Technology, ehale@mst.edu

Thomas J. O'Keefe
Missouri University of Science and Technology

Y. M. Wang

et. al. For a complete list of authors, see https://scholarsmine.mst.edu/phys_facwork/2620

Recommended Citation

D. Abayarathna et al., "Effects Of Sample Orientation On The Corrosion Of Zinc In Ammonium Sulfate And Sodium Hydroxide Solutions," *Corrosion Science*, vol. 32, no. 7, pp. 755 - 768, Elsevier, Jan 1991.
The definitive version is available at https://doi.org/10.1016/0010-938X(91)90089-8

Corrosion Science, Vol. 32, No. 7, pp. 755–768, 1991
Printed in Great Britain.

0010–938X/91 $3.00 + 0.00

EFFECTS OF SAMPLE ORIENTATION ON THE CORROSION OF ZINC IN AMMONIUM SULFATE AND SODIUM HYDROXIDE SOLUTIONS

D. ABAYARATHNA,* E. B. HALE,* T. J. O'KEEFE,* Y.-M. WANG† and D. RADOVIC†

*Graduate Center for Materials Research, University of Missouri-Rolla, Rolla, MO 65401, U.S.A.
†Physical Chemistry Department, General Motors Research Laboratories, Warren, MI 48090, U.S.A.

Abstract—The corrosion and electrochemical properties of three zinc single crystal surfaces with different orientations have been investigated. In near-neutral 1 M $(NH_4)_2SO_4$, the corrosion rates on all three surfaces were found to be similar. However, the SEM morphologies of the corresponding corroded surfaces were markedly different from each other, but consistent with preferential attack of $\{11\bar{2}0\}$ surfaces. In alkaline 0.5 N NaOH solution, the three sample orientations showed significantly different reactivities, with the $(11\bar{2}0)$ surface exhibiting the highest reactivity and corrosion rate. Here, passivation ultimately occurred and the difference in the corrosion performance of the three surfaces, even for small overvoltages, is attributed to the presence of oxide or hydrated oxide films.

INTRODUCTION

ZINC has been effectively employed in the galvanic protection of steel for many decades. Zinc utilization has been on the increase partially because of the trend to extended warranties and guarantees against car body deterioration. In addition to the traditional hot-dip coating process, increased tonnage of electro-galvanized products is now being supplied as well. In spite of the major importance that the corrosion properties of zinc has in such applications, there are few fundamental studies on the corrosion of zinc which focus on the influence of orientation and morphology. To further the understanding of zinc corrosion, a collaborative research project has been carried out at the University of Missouri-Rolla (UMR) and at the General Motors Research Laboratories (GMR).

Since electrogalvanized coating may be deposited with preferred orientations, it seemed reasonable to first examine the corrosion properties of various crystallographically oriented surfaces of high purity zinc single crystals. This study focussed on the electrochemical behavior of zinc in two distinctly different media, which were near-neutral and strongly alkaline in nature. The near-neutral media studies were made in $(NH_4)_2SO_4$ solutions with an initial pH of 6 by the UMR group. The GMR group made the alkaline media studies using 0.5 N NaOH solution. Both oxygen-saturated and nitrogen-sparged $(NH_4)_2SO_4$ solutions were used. Most of the studies were done in the nitrogen sparged solutions since they are known to suppress oxide film formation on zinc surfaces.[1,2] In addition, they yielded more reproducible results. The NaOH solution was used because the corrosion environment at the metal/paint interface is usually alkaline in nature. It is also established that zinc passivates in alkaline solutions[3] and zinc oxide/hydroxide films are known to play an important role in the zinc corrosion process.[4,5]

Manuscript received 14 August 1989; in amended form 26 August 1990.

The corrosion behavior was investigated using d.c. polarization measurements and morphological information obtained from scanning electron micrographs. Corrosion rate assessments were made from Tafel slope extrapolations and calculations using Tafel slopes and the polarization resistance.

EXPERIMENTAL METHOD

Sample preparation

The single crystal zinc samples used in these investigations had a purity of 99.999% and were provided by Cominco Ltd, Trail, British Columbia. A spark cutter was used to provide samples which had their largest surface parallel to a (0001), $(10\bar{1}0)$ or $(11\bar{2}0)$ plane. These orientations were confirmed by Laue back reflection and X-ray diffraction. The average deviation of the surface from its desired plane was $\pm 1°$ with a maximum deviation of 3°.

Samples were mounted using epoxy (Quickmount) and mechanically polished by wet grinding on silicon carbide paper. Reproducible, very smooth, and mirror-like sample surfaces were obtained using slightly different procedures at UMR and GMR laboratories. At UMR, ultrasonic rinsing and final mechanical polishing with alumina of 1 and 0.3 μm size was done. The samples were cleaned ultrasonically again and then rinsed with a stream of de-ionized water. Surfaces were dried with nitrogen gas and the edges were masked with electroplaters', tape so as to expose an area of 0.50 cm^2. The electrodes were then anodically polished for 30 min in a solution of 40% (by volume) orthophosphoric acid and 60% denatured ethanol at room temperature. The cell voltage was maintained at 2.0 V and the corresponding current density was 10.0 mA cm^{-2}. The electrodes were rinsed thoroughly in de-ionized water immediately after electropolishing and transferred wet into the test cell. At GMR, samples were first wheel-polished with 5 and 0.3 μm alumina paste and ultrasonically cleaned in distilled water. The samples were then chemically etched in 8 N HNO_3 for 2 s and electropolished at 0.050 V with respect to a SEC (saturated calomel electrode) in a 1:1 absolute ethanol–concentrated orthophosphoric acid mixture until a total charge passage of 10 C cm^{-2} occurred. Distilled water rinses were incorporated between each step.

Procedures

Measurements in $(NH_4)_2SO_4$ *solutions.* The corrosion measurements were carried out in a one liter glass electrochemical cell with a platinum mesh counter electrode and a saturated calomel reference electrode. The electrolyte was unbuffered and was either aerated or de-aerated 1 M $(NH_4)_2SO_4$ at 25 ± 2°C. In the aerated solutions, oxygen was continuously bubbled through the electrolyte, while the de-aerated solutions were maintained by continuously bubbling nitrogen through the electrolyte. To determine the cathodic and anodic corrosion behavior, potentiodynamic scans were made using a Petrolite Model M-4100 Potentiodyne Analyzer.

To begin the corrosion testing, a sample was introduced into the cell immediately after electropolishing and allowed to come to equilibrium, which usually took 15 min. After the potential stabilized, the open circuit potential (E_{corr}) was recorded. Current–potential data for determination of the polarization resistance were then taken. First, the potential was adjusted to 5.0 mV negative to the corrosion potential and scanning was initiated in the anodic direction at a rate of 0.1 mV s^{-1}. Current measurements were taken at 1 mV intervals up to a potential which was 5.0 mV positive to E_{corr}. From these data, the polarization resistance R_p was obtained by taking the slope of the E vs i curve at E_{corr}.

To take the Tafel region data, the open circuit potential was allowed to re-stabilize. Then, a cathodic potential sweep starting at E_{corr} was carried out at a rate of -0.25 mV s^{-1}, a sweep rate which was slow enough to provide reproducible curves. When a current density of 2 mA cm^{-2} was obtained, the applied voltage was removed and the potential was allowed to re-stabilize so that the new E_{corr} could be determined. The new value of E_{corr} was always within 10 mV of the original value and usually closer. Finally, the anodic sweep was made starting from E_{corr} at a rate of $+0.25$ mV s^{-1}.

Measurements in NaOH *solutions.* The electrolyte, 0.5 N NaOH with a pH of 13.5, was initially zincate-free and de-aerated by purging with pre-purified nitrogen. The cell used was an acrylic 'H' cell with a platinum mesh counter electrode and a saturated calomel reference electrode. All measurements were made by a computer controlled PAR Model 332-1 Corrosion Measurement System.

The zinc sample was immersed in solution at an applied potential of -1.8 V(SCE) for 5 min to generate a more reproducible surface. After this cathodic pre-polarization step, the electrode was left at open

circuit for 5 min to establish the corrosion potential. The applied potential began at −1.9 V and was swept in the anodic direction to +1.0 V. Various sweep rates were used to determine an optimum rate that would provide reproducible polarization curves and minimize surface changes. A sweep rate of 10 mV s^{-1} gave the most satisfactory results.

First, the polarization resistance was determined by making measurements in the ±10 mV region around E_{corr}. Then, a more extensive sweep was made to obtain data in the Tafel regions. To examine the passivation process, some anodic sweeps were extended out until passivation occurred.

Morphological studies. Scanning electron microscopy (SEM) photographs were taken to examine the morphology of the corroded surfaces. The surfaces of the samples were water rinsed after corrosion testing and then observed without further treatment.

EXPERIMENTAL RESULTS

d.c. Polarization studies

$(NH_4)_2SO_4$ solution. Figure 1 shows typical polarization curves obtained in aerated (oxygen saturated) or de-aerated (nitrogen sparged) $(NH_4)_2SO_4$ solutions on (0001) oriented surfaces. The de-aerated solutions gave curves which showed well defined Tafel regions in both the anodic and cathodic sweeps. In the aerated solutions, no extended linear regions were found in the cathodic curve, as expected. Thus, most of our measurements were made in de-aerated solutions.

More details on the anodic and cathodic regions for variously oriented surfaces are shown in Figs 2 and 3. The anodic behavior was almost identical for the three planes considered, but the (0001) surfaces yielded slightly greater current densities at a given cathodic overvoltage.

The polarization measurements were analysed using mixed potential theory developed for simultaneous corrosion reactions.[6,7] Slopes in the anodic (b_a) and cathodic (b_c) Tafel regions were obtained from a computer fit to the data. The results given in Table 1 are the average of measurements made on three samples for each of the three orientations. The table also shows the average values for the corrosion potential and the polarization resistance R_p obtained from the slope of the low overvoltage E–i curve at E_{corr}.[8] These data clearly show the similarity of the three orientations in their anodic and cathodic behaviors. However, there are

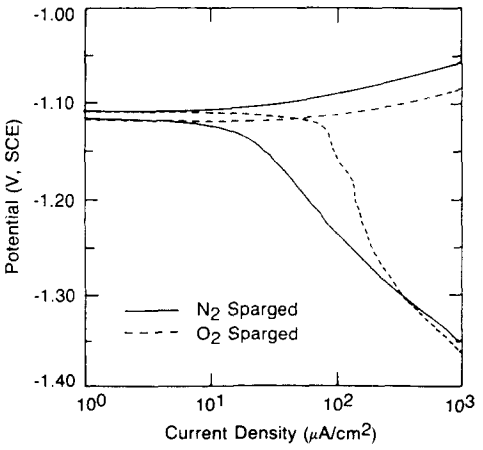

FIG. 1. Polarization curves from a (0001) surface in nitrogen or oxygen saturated 1 M $(NH_4)_2SO_4$.

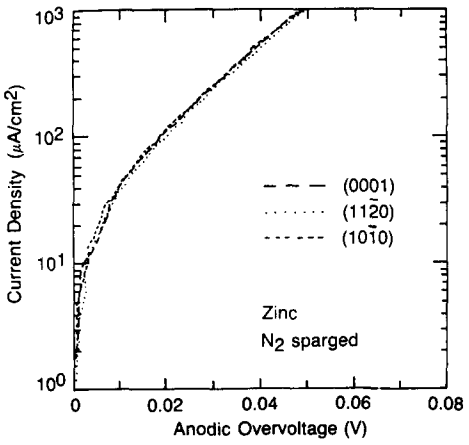

FIG. 2. Anodic Tafel plots from (0001), (10$\bar{1}$0) and (11$\bar{2}$0) surfaces in de-aerated 1 M $(NH_4)_2SO_4$.

noticeable differences in E_{corr} and R_p between the (0001) orientation and the (10$\bar{1}$0) or (11$\bar{2}$0) orientations. Thus, there is probably a slightly different reaction or a film forming on the (0001) surface which Fig. 3 suggests is predominantly at low overvoltages.

The anodic and cathodic current densities at E_{corr} (i^a_{corr} and i^c_{corr}) were determined from Tafel slope extrapolation back to E_{corr}. In addition, corrosion currents were also calculated using the Tafel slopes (b_a and b_c) and polarization resistance (R_p) in the equation of Stern and Geary,[9,10] i.e.

$$i^{R_p}_{corr} = b_a b_c / 2.303\,(b_a + b_c) R_p. \tag{1}$$

The results for the three methods used to obtain the corrosion currents are given in Table 2. The three methods yielded slightly different results. The differences in the three corrosion currents for the same orientation may be more a result of the testing procedures, such as changes in sample surface area during the experiment or initial

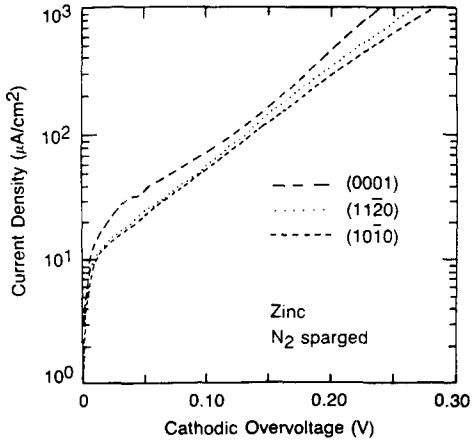

FIG. 3. Cathodic Tafel plots from (0001), (10$\bar{1}$0) and (11$\bar{2}$0) surfaces in de-aerated 1 M $(NH_4)_2SO_4$.

TABLE 1. ELECTROCHEMICAL PARAMETERS FOR (0001), $(10\bar{1}0)$ AND $(11\bar{2}0)$ ZINC SURFACES IN DE-AERATED 1 M $(NH_4)_2SO_4$ SOLUTIONS. THE OPEN CIRCUIT POTENTIAL, TAFEL SLOPES, AND POLARIZATION RESISTANCE WERE OBTAINED DIRECTLY FROM THE POLARIZATION CURVES

Exposed surface	E_{corr} [V(SCE)]	b_a (mV)	b_c (mV)	R_p (Ω cm^2)
(0001)	−1.116	31	124	1052
$(10\bar{1}0)$	−1.132	31	132	1447
$(11\bar{2}0)$	−1.132	32	127	1499

TABLE 2. CORROSION RATES FOR (0001), $(10\bar{1}0)$ AND $(11\bar{2}0)$ ZINC SURFACES IN 1 M $(NH_4)_2SO_4$ SOLUTIONS. THESE RATES WERE DETERMINED FROM TAFEL SLOPE EXTRAPOLATIONS AND THE STERN AND GEARY EQUATION

Exposed surface	i^a_{corr} (μA cm^{-2})	i^c_{corr} (μA cm^{-2})	$i^{R_p}_{corr}$ (μA cm^{-2})
(0001)	19	8.6	10.3
$(10\bar{1}0)$	27	9.1	7.5
$(11\bar{2}0)$	23	9.3	7.2

polarity of polarization, than any real differences. However, the differences and trend among the surface orientations are thought to be reliable since the (0001) orientation is clearly different from the $(10\bar{1}0)$ or $(11\bar{2}0)$ orientation, which are similar.

Alkaline solution. A typical polarization curve obtained from a (0001) surface in de-aerated 0.5 N NaOH solution is shown in Fig. 4. In the cathodic sweep, a Tafel

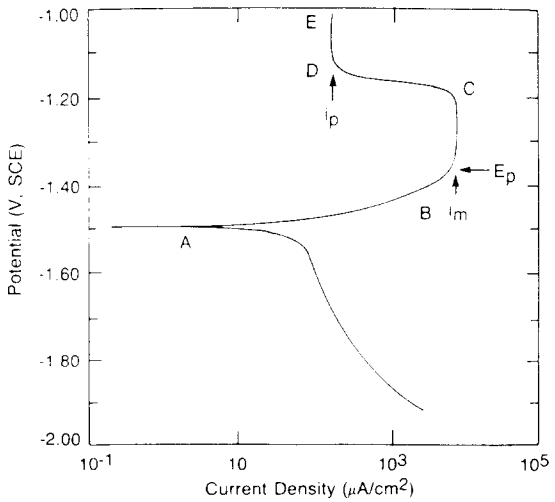

FIG. 4. Polarization curve from a (0001) surface in 0.5 N NaOH at a 10 mV s^{-1} scan rate.

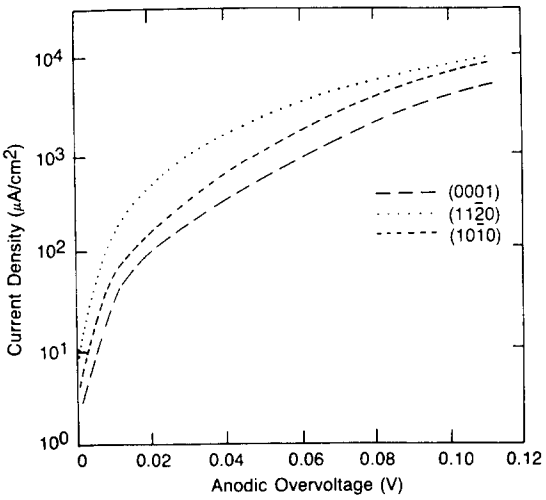

FIG. 5. Anodic Tafel plots from (0001), (10$\bar{1}$0) and (11$\bar{2}$0) surfaces in 0.5 N NaOH.

region was observed. In the anodic sweep, the polarization curve is much more complex and constant current regions in the current density suggest that film formation is clearly occurring.

More detailed anodic and cathodic results for different orientations are shown in Figs 5 and 6. In contrast to the near-neutral solution results, the curves generated using the three orientations were clearly different. The anodic plots showed that, for a given overvoltage, the reaction current density was least on the (0001) surface and greatest on the (11$\bar{2}$0) surface. Both the (0001) and (10$\bar{1}$0) surfaces appear to exhibit Tafel behavior over one decade of current density, whereas on the (11$\bar{2}$0) surface no clear Tafel region was observed. The cathodic Tafel plots also showed a surface

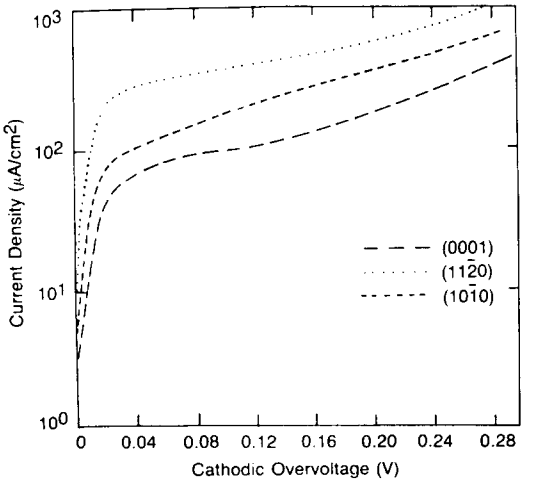

FIG. 6. Cathodic Tafel plots from (0001), (10$\bar{1}$0) and (11$\bar{2}$0) surfaces in 0.5 N NaOH.

orientation dependence, which for a given overvoltage, again showed the (0001) surface to yield the lowest current density, while the $(11\bar{2}0)$ surface had the highest.

The polarization data for each orientation were used to obtain Tafel slopes and polarization resistances. For this analysis the Tafel slopes were obtained by graphical extrapolation, as were E_p, the passivation potential, i_m, the maximum current density, and i_p, the current density in the passive region, as shown in Fig. 4. Electrochemical parameters for the three orientations studied are summarized in Table 3. The Tafel slopes were similar for the three surfaces in the anodic region, but were different in the cathodic region. The first plateau region occurred at a much lower voltage and current density on the (0001) surface than on the other two surfaces. The polarization resistances of the (0001) and $(10\bar{1}0)$ surfaces were similar, whereas that of the $(11\bar{2}0)$ surface had a much lower value. It appears that the oxide/hydroxide film which formed on the (0001) surfaces was the most protective since it exhibited the lowest leakage current density.

The corrosion currents were calculated from anodic and cathodic Tafel slope extrapolations, as well as from the Stern and Geary equation. These results are shown in Table 4. The results from the different calculations were not very consistent but are useful to indicate relative differences. There were variations among the three orientations with a much greater current density determined on the $(11\bar{2}0)$ surface and lowest current density on the (0001) surface.

Morphological studies results. For any given orientation, the surfaces observed after corrosion testing were similar in either test solution used in this study. Morphological studies made on the three orientations after corrosion tests showed

TABLE 3. ELECTROCHEMICAL PARAMETERS FOR (0001), $(10\bar{1}0)$ AND $(11\bar{2}0)$ ZINC SURFACES IN DE-AERATED 0.5 N NaOH SOLUTION. THE OPEN CIRCUIT POTENTIAL, PASSIVATION POTENTIAL, MAXIMUM CURRENT DENSITY, CURRENT DENSITY IN THE PASSIVE REGION, TAFEL SLOPES, AND POLARIZATION RESISTANCE WERE OBTAINED DIRECTLY FROM THE POLARIZATION CURVES

Exposed surface	E_{corr} [V(SCE)]	E_p [V(SCE)]	i_m (μA cm^{-2})	i_p (μA cm^{-2})	b_a (mV)	b_c (mV)	R_p (Ω cm^2)
(0001)	−1.465	−1.298	9609	204	43	421	285
$(10\bar{1}0)$	−1.472	−1.332	15446	581	40	368	234
$(11\bar{2}0)$	−1.455	−1.320	16573	605	38	512	63

TABLE 4. CORROSION RATES FOR (0001), $(10\bar{1}0)$ AND $(11\bar{2}0)$ ZINC SURFACES IN 0.5 N NaOH SOLUTION. THESE RATES WERE DETERMINED FROM TAFEL SLOPE EXTRAPOLATIONS AND THE STERN AND GEARY EQUATION

Exposed surface	i^a_{corr} (μA cm^{-2})	i^c_{corr} (μA cm^{-2})	$i^{R_p}_{corr}$ (μA cm^{-2})
(0001)	34	60	60
$(10\bar{1}0)$	53	101	68
$(11\bar{2}0)$	235	278	243

quite distinct differences. Corroded basal plane always showed hexagonal pitting with the facets of the hexagons being parallel to $\{10\bar{1}0\}$ planes (see Fig. 7). On the other hand, a striated structure was present on corroded $(10\bar{1}0)$ planes (see Fig. 8a). The well oriented, elongated striations were parallel to (0001) planes and were more pronounced when the surface is viewed from off normal directions as in Fig. 8(b) and (c). The morphology of the corroded $(11\bar{2}0)$ face shown in Fig. 9(a) seemed to indicate an irregular type of corrosion, but closer examinations after tilting the sample revealed an oriented, crested ridge structure (see Fig. 9b and c). The surface structures on all three orientations were very reproducible and strongly orientation dependent. Some morphology studies were done on samples left immersed in the electrolyte for several hours without any voltage being applied. These open-circuit studies also indicated a clear orientation dependence.

DISCUSSION

Reactions in $(NH_4)_2SO_4$ *solutions*

Three possible reactions occurring during the anodic dissolution of zinc are:

$$Zn \rightarrow Zn^+ + e^- \tag{2}$$

$$Zn^+ \rightarrow Zn^{2+} + e^- \tag{3}$$

and

$$Zn^{2+} + H_2O \rightarrow ZnOH^+ + H^+. \tag{4}$$

For all three orientations, the anodic Tafel slope was determined to be about 30 mV decade^{-1} in the $(NH_4)_2SO_4$ solutions. If the rate determining step is reaction (4) or any similar chemical step, then the expected anodic Tafel slope is 30 mV decade^{-1}.[11] However, if the rate determining step is reaction (3), then the expected slope is 40 mV decade^{-1}.[11] This latter value is typically the result found in most other zinc studies which were all on polycrystalline zinc. For example, Baugh[2] studied polycrystalline zinc samples in various media, including $(NH_4)_2SO_4$, and obtained slopes near 40 mV decade^{-1}.

Similar measurements were also made on polycrystalline galvanized wires in $(NH_4)_2SO_4$ solution and a slope of 40 mV decade^{-1} was found. It appears that on the single crystal surfaces the formation of $ZnOH^+$ is significantly more inhibited than in other zinc corrosion cases. This suggests grain boundaries or perhaps multiple exposed orientations greatly promote reaction (4) and thus reaction (3) becomes the rate determining step. In the alkaline solutions, where ZnOH can readily form, a 40 mV decade^{-1} slope was measured. Hence, a slope of 30 or 40 mV decade^{-1} is obtained depending on the nature of the zinc surface.

The cathodic polarization measurements on $(10\bar{1}0)$ and $(11\bar{2}0)$ surfaces in the

FIG. 7. SEM micrograph of corroded (0001) surface in de-aerated 1 M $(NH_4)_2SO_4$.

FIG. 8. SEM micrographs of corroded $(10\bar{1}0)$ surface in de-aerated 1 M $(NH_4)_2SO_4$. (a) Normal view with sample in the x–y plane where x and y axes were parallel to $[11\bar{2}0]$ and [0001] directions, respectively, and beam was along z axis and parallel to $[10\bar{1}0]$. (b) View with sample tilted 45° about x axis. (c) View with sample rotated 90° about z axis and tilted 45° about x axis.

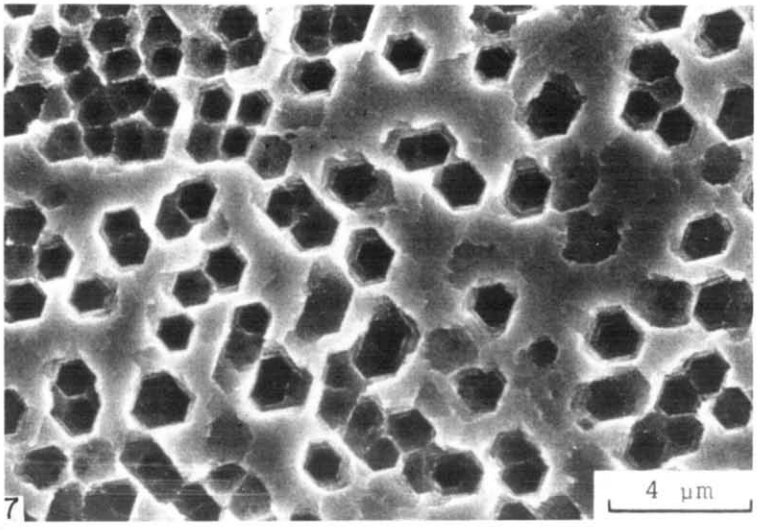
7
4 μm

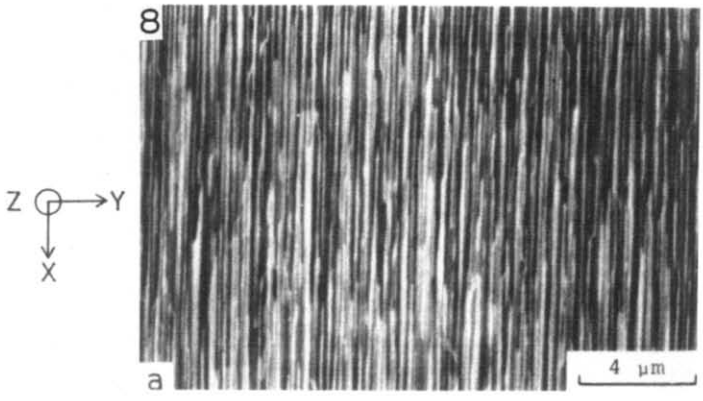
8
Z
Y
X
a
4 μm

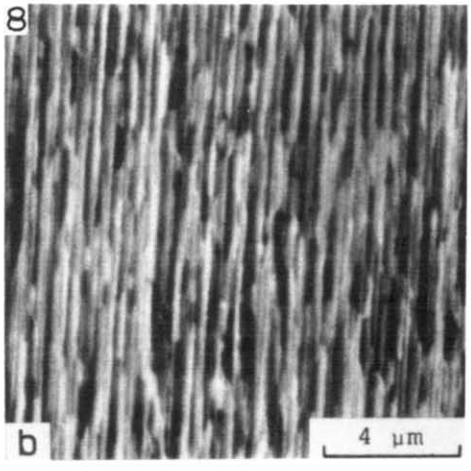
8
b
4 μm

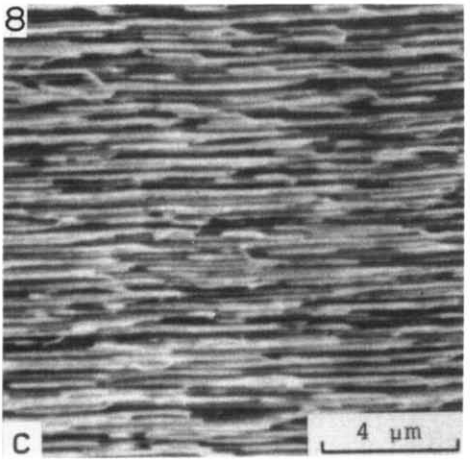
8
c
4 μm

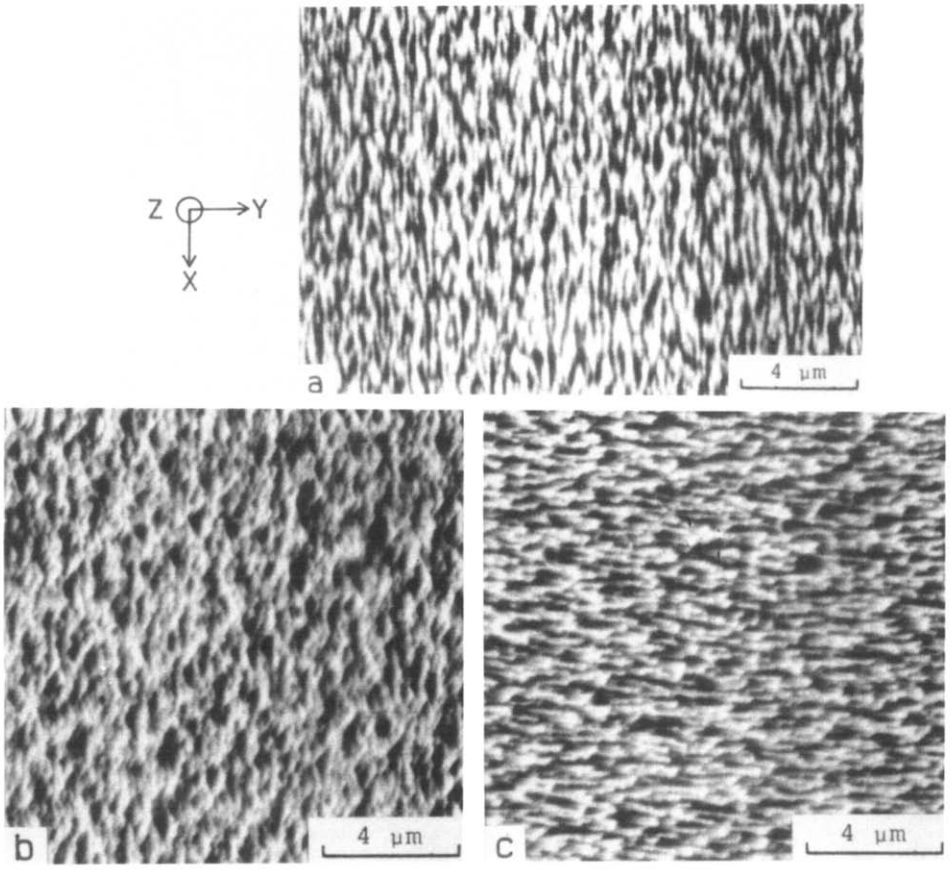

FIG. 9. SEM micrographs of corroded $(11\bar{2}0)$ surface in de-aerated 1 M $(NH_4)_2SO_4$. (a) Normal view with sample in the x–y plane where x and y axes were parallel to $[\bar{1}100]$ and [0001] directions, respectively, and beam was along z axis and parallel to $[11\bar{2}0]$. (b) View with sample tilted 45° about x axis. (c) View with sample rotated 90° about z axis and tilted 45° about x axis.

$(NH_4)_2SO_4$ solution were rather similar and showed linear regions. The Tafel slopes were found to be about 130 mV decade^{-1}. The (0001) surface also had a linear region, but only at the higher overpotentials. A slope of 120 mV decade^{-1} is expected for hydrogen evolution when electron transfer reaction is the rate determining step.[11]

Reactions in NaOH *solutions*

Sergi *et al.*[5] have reported an oxide or hydrated oxide was found to form on zinc when immersed in sodium hydroxide solution. The coverage of the oxide film can be complete or patchy, and that could affect the corrosion behavior of the underlying zinc. The results indicated that the coverage of the oxide is most complete on the (0001) surface since it has the highest R_p value and lowest i_{corr} value. The $(10\bar{1}0)$ surface film is less protective according to the Tafel slope determined i_{corr} value even though its value was about the same as for the (0001) surface. The least protective surface was clearly the $(11\bar{2}0)$ surface film which had a much lower R_p value and definitely the highest i_{corr}.

The presence of oxide films makes precise analysis of the electrokinetic measurements very difficult. The results clearly show that the corrosion rate and passivation behavior of zinc under both anodic and cathodic sweeps depend on surface orientation. These polarization measurements showed the relative corrosion behavior of the overvoltages used in the R_p studies. Namely, the corrosion rates were greatest on the $(11\bar{2}0)$ surface and least on the (0001) surface. These results suggest that the initially formed oxide film has a long lasting effect in controlling the corrosion behavior.

The anodic polarization curves were observed to be very non-linear and complex, probably due to the formations of oxidative films as can be seen in Fig. 4. Region AB in Fig. 4 has been attributed[3] to the active dissolution of zinc: $Zn + 4(OH)^- = Zn(OH)_4^{-2} + 2e^-$.

When the zincate concentration at the zinc surface reaches a critical value corresponding to supersaturation, an insoluble salt, either ZnO or $Zn(OH)_2$, precipitates onto the surface and creates the plateau region BC, where the current density remains relatively constant for 200 mV. The independence of current density from the applied voltage suggests that the zinc oxide/hydroxide film formed in this region is non-protective and the film formation is a mass transport related process. At point C, the current density suddenly decreases with increasing voltage and signals the onset of zinc passivation. Region DE represents the passive region for zinc.

The cathodic Tafel slopes are attributed to hydrogen evolution as were those from the $(NH_4)_2SO_4$ solution results. In this case the slopes are much larger because of the presence of two simultaneous cathodic reactions:

$$2H_2O + 2e^- = 2(OH)^- + H_2, \tag{5}$$

and

$$2H^+ + 2e^- = H_2. \tag{6}$$

Reaction (5) is activation controlled with a Tafel slope of 120 mV decade^{-1}. Reaction (6) is diffusion controlled with a Tafel slope of infinity in strong alkaline solutions.

Corrosion current density

The corrosion current densities calculated by the three different methods were not very similar (see Tables 2 and 4). In particular, the current density values deduced from the anodic Tafel extrapolation in the $(NH_4)_2SO_4$ corrosion tests were much higher than those deduced from the cathodic results. One possible cause of this observation is that the corrosion rate depends on the previous polarization history of the sample. To examine this possibility, the sweeps to obtain the polarization resistance and the anodic region behavior were *not* made on several samples. Instead, three repetitive cathodic polarization measurements were made on samples which were allowed to stabilize between sweeps. Each run yielded an increasing cathodic current density relative to the previous run. This suggests that some, if not most, of the differences between the corrosion current densities in Tables 2 and 4 were due to the sweep procedures used in the tests. However, since a standard sweep procedure was used for all tests, it is believed that the relative differences between samples is meaningful.

Preferential corrosion

The morphological studies on samples corroded in the $(NH_4)_2SO_4$ solution revealed the strong influence of crystallographic orientation on the nature of the attack. A preferential atomic layer type of attack is clearly indicated. This type of corrosion is comparable to the reverse of single crystal deposition and growth—a process which has been studied and analysed by several groups.[12–16] In the present case, the morphology of the three differently oriented surfaces was clearly different. However, the polarization measurements show relatively subtle differences (see Figs 2 and 3). Corrosion is initiated at some activated site. On a (0001) face, for example, preferential atomic attack causes well defined hexagonal etch pits to form on the surface (see Fig. 7) and, on a macroscopic scale, reveals the basal plane symmetry of this surface. The facets of these pit walls are parallel to $\{10\bar{1}0\}$ planes. Such a geometrical configuration is expected if the corrosive attack was highest on $\{11\bar{2}0\}$ planes. In such a case, $\{11\bar{2}0\}$ planes dissolve preferentially leaving behind $\{0001\}$ surfaces.

Corrosion of a $(10\bar{1}0)$ surface reveals well aligned striations (see Fig. 8). These striations are parallel to a (0001) plane and hence are edges of basal planes. This result suggests that the basal plane is the least active plane as might have been inferred from the micrographs of the corroded (0001) surface where much of the surface still appeared smooth and not radically altered by the polarization test. In contrast, all the $(10\bar{1}0)$ surfaces appear heavily attacked and well defined $(11\bar{2}0)$ or $(10\bar{1}0)$ planes were not seen.

Viewing a corroded $(11\bar{2}0)$ surface, as in Fig. 9, shows a seemingly less symmetric situation. However, by tilting the sample 45° relative to the $[11\bar{2}0]$ direction a more laminar structure with some well defined ridges can be seen. Here again the laminar structure left behind was parallel to a (0001) plane further indicating the stability of the basal planes.

Although the morphologies appear quite different when the different surface orientations are viewed, they are all consistent with preferential attack on $(11\bar{2}0)$ planes with the attack on the (0001) planes being consistently lower.

In the alkaline solution, the anodic polarization measurements showed the highest corrosion rates on the $(11\bar{2}0)$ surfaces and lowest on the (0001) surfaces. The

appearance of the corroded surfaces are similar to those observed in the $(NH_4)_2SO_4$ medium and are consistent with the corrosion rate data.

Ashton and Hepworth[17] have also reported measurements on single crystal zinc in alkaline solutions. They indicated that the anodic overvoltages decreased in the order (0001), $(10\bar{1}0)$, and $(11\bar{2}0)$, and the $(11\bar{2}0)$ face showed the highest corrosion rate, followed by $(10\bar{1}0)$, then (0001). The corrosion rate measurements in NaOH solutions confirmed their relative results among the three orientations. They associated the differences in corrosion rates with the differences in planar packing density. The activation energy for dissolution was suggested to increase as the packing density increased. In such a case, the face with the highest packing density should have the lowest corrosion rate. This theory might explain why the (0001) orientation has the lowest corrosion rate since this plane does have the highest packing density. However, the packing density of zinc decreases in the order: $\rho_{(0001)} > \rho_{(11\bar{2}0)} > \rho_{(10\bar{1}0)}$.[16] Therefore, packing density cannot explain the fact that the corrosion rate is higher for $(11\bar{2}0)$ surfaces than for $(10\bar{1}0)$ surfaces as observed here, as well as by Ashton and Hepworth.[17] The results from the alkaline solution testing very clearly show that the reactivity of zinc varies with crystal face. The reactivity is clearly greatest on a $(11\bar{2}0)$ face. Some self-passivation occurred on the zinc surface, the face with the ability form the most protective oxide film is the least active.

CONCLUSION

Corrosion studies on single crystal zinc samples with surfaces oriented parallel to (0001), $(10\bar{1}0)$, or $(11\bar{2}0)$ crystallographic planes were carried out. Studies were done in near neutral media, 1 M $(NH_4)_2SO_4$, where film formation appears to be weak, if present at all, and in strongly alkaline media, 0.5 N NaOH, where clear evidence of film formation was observed.

In the near neutral solutions, the polarization curves taken on all three surface orientations were rather similar, but the physical appearance of the three surfaces was radically different. The three surfaces all had structural aspects related to the underlying crystal structure. Corrosion on the basal plane resulted in hexagonal pits with facets parallel to $\{10\bar{1}0\}$ planes. On $(10\bar{1}0)$ oriented surfaces, elongated striated structures were observed with the elongation aligned along the $[10\bar{1}0]$ direction. Corrosion on $(11\bar{2}0)$ surfaces resulted in a crested ridge structure.

The observed surface features of all three surface orientations indicated that the corrosive attack was predominantly on $\{11\bar{2}0\}$ surfaces and least on $\{0001\}$ surfaces. In addition, regardless of initial surface orientation, the results of corrosion changed the morphology to be consistent with $\{11\bar{2}0\}$ being the most active face. Thus, from a mechanistic standpoint, the nature of the surface bonding and resulting film formation and chemical activity causes this face to be the dominant one during the dissolution process. Such processes dominate since the results are not directly related to packing density, as was previously inferred.

Further studies should reveal the relevance of this work to electrogalvanized coatings. Preliminary results on galvanized coatings have shown that on a microscopic scale the localized corrosion morphology follows the same structural patterns seen in this study on single crystal surfaces. Individual facets within a polycrystalline coating corrode with different morphologies with, for example, basal plane pits clearly seen on some facets and striations on others. Of potentially greater relevance has been the observation that the rather subtle corrosion rate differences found

between different orientations in this study have more pronounced effects in polycrystalline zinc. This is because all facets assume the same corrosion potential which means the corrosion rate is least on basal plane facets and these facets showed less degradation. In practice, evaluating corrosion effects is likely to be more complex than in pure zinc because commercial coatings usually require a phosphate conversion coating and are painted. Additional research is required on such complex multi-layer coatings before a definitive answer can be obtained as to the actual and most desirable effect of zinc surface orientation on actual corrosion during atmospheric exposure.

In the 0.5 N NaOH solutions the presence of strong surface orientation effects was seen directly in the polarization measurements. The corrosion rate was greatest on $\{11\bar{2}0\}$ surfaces. These rates were in the same relative order as those found in the near neutral media. This agreement may be fortuitous since film formation clearly had a great influence on the polarization measurements in the alkaline solution. The oxide or hydrated oxide film which formed on the (0001) surface appeared to be the most protective.

Acknowledgements—The authors wish to thank Cominco Ltd, Trail, British Columbia for providing materials, Marion Dattilo of U.S. Bureau of Mines for valuable technical assistance and discussion, and Dr James W. Johnson of the Chemical Engineering Department at UMR for helpful suggestions related to this study.

REFERENCES

1. L. M. BAUGH, *Electrochim. Acta* **24**, 657 (1979).
2. L. M. BAUGH, *Electrochim. Acta* **24**, 669 (1979).
3. L. M. BAUGH and A. HIGGINSON, *Electrochim. Acta* **30**, 1163 (1985).
4. HEIDHEISER, Jr and I. SUZUKI, *J. electrochem. Soc.* **128**, 242 (1981).
5. G. SERGI, N. R. SHORT and C. L. PAGE, *Corrosion* **41**, 619 (1985).
6. C. WAGNER and W. TRAUD, *Z. Electrochem.* **44**, 391 (1938).
7. J. V. PETROCELLI, *J. Electrochem.* **97**, 10 (1950).
8. K. B. OLDHAM and F. MANSFELD, *Corrosion* **27**, 434 (1971).
9. M. STERN and A. L. GEARY, *J. electrochem. Soc.* **104**, 56 (1957).
10. M. STERN, *J. electrochem. Soc.* **104**, 645 (1957).
11. J. O'M. BOCKRIS and A. K. N. REDDY, *Modern Electrochemistry*, Vol. 2, Chapter 9. Plenum, New York (1973).
12. J. O'M. BOCKRIS and A. K. N. REDDY, *Modern Electrochemistry*, Vol. 2, Chapter 10. Plenum, New York (1973).
13. *Growth and Perfection of Crystals* (eds R. H. DOREMUS, B. W. ROBERTS and DAVID TURNBULL. John Wiley, New York (1958).
14. M. FLEISHMANN and H. R. THIRSK, *Adv. Electrochem. Electrochem. Engng* **3**, 123 (1958).
15. A. DAMJANOVIC, *Modern Aspects of Electrochemistry*. Butterworth, London (1964).
16. R. SATO, *J. electrochem. Soc.* **106**, 206 (1959).
17. R. F. ASHTON and M. T. HEPWORTH, *Corrosion* **24**, 50 (1968).